AD A037496

SECURITY CLASSIFICATION OF THIS PAGE (When Data Entered)

REPORT DOCUMENTATION PAGE

READ INSTRUCTIONS BEFORE COMPLETING FORM

1. REPORT NUMBER	2. GOVT ACCESSION NO.	3. RECIPIENT'S CATALOG NUMBER

4. TITLE (and Subtitle)
MECHANISMS, BRANCHING RATIOS AND RATE CONSTANTS FOR EXCITATION PROCESSES IN RARE GAS SYSTEMS.

5. TYPE OF REPORT & PERIOD COVERED
ANNUAL TECHNICAL REPORT, January 1976 - January 1977

6. PERFORMING ORG. REPORT NUMBER

7. AUTHOR(s)
D. W. Setser

8. CONTRACT OR GRANT NUMBER(s)
N00014-76-C-0380
ARPA Order-2840

9. PERFORMING ORGANIZATION NAME AND ADDRESS
D. W. Setser
Chemistry Department, Kansas State University
Manhattan, Kansas 66506

10. PROGRAM ELEMENT, PROJECT, TASK AREA & WORK UNIT NUMBERS
ARPA Order No. 284014
Program Code 421

11. CONTROLLING OFFICE NAME AND ADDRESS
Advanced Research Projects Agency
1400 Wilson Boulevard
Arlington, Va. 22209

12. REPORT DATE
January, 1977

13. NUMBER OF PAGES
33

14. MONITORING AGENCY NAME & ADDRESS (if different from Controlling Office)
Physics Program
Office of Naval Research
800 N. Quincy Ave.
Arlington, Va. 22217

15. SECURITY CLASS. (of this report)
Unclassified

15a. DECLASSIFICATION/DOWNGRADING SCHEDULE

16. DISTRIBUTION STATEMENT (of this Report)
Approved for public release; distribution unlimited

DDC RECEIVED MAR 29 1977 C

17. DISTRIBUTION STATEMENT (of the abstract entered in Block 20, if different from Report)

18. SUPPLEMENTARY NOTES

19. KEY WORDS (Continue on reverse side if necessary and identify by block number)
Rare gas metastable atoms, quenching rate constants, product branching fractions, Penning ionization.

20. ABSTRACT (Continue on reverse side if necessary and identify by block number)
The work done with support from this contract can be divided into three categories:

1. Measurement of total quenching rate constants and branching fractions for krypton halide formation for metastable krypton atoms reacting with halogen containing molecules. The decay rates of $Kr(^3P_2)$ and $Xe(^3P_2)$ in pure argon also has been studied.

DDC FILE COPY

DD FORM 1 JAN 73 1473 EDITION OF 1 NOV 65 IS OBSOLETE

400867

SECURITY CLASSIFICATION OF THIS PAGE (When Data Entered)

20. Continued

2. ~~II~~. Construction of an apparatus which will permit the measurement of the rate constants for electronic excitation of products resulting from charge transfer reactions of He_2^*. These charge transfer reactions will be compared to the Penning ionization reactions of $He(2^3S)$ atoms; some data already have been acquired for the latter.

3. ~~III~~. Investigation of the applicability of the ionic-covalent curve-crossing mechanism for the formation of Br_2^*, I_2^* and other excited states of molecular halogens that have been demonstrated to be candidates for U.V. lasers.

All of this work is directed toward discovery of new excitation processes in electrically pumped rare gases that might lead to new visible and U.V. lasers or to measurement of kinetic data that will be of value to modeling calculations for known laser systems.

ANNUAL TECHNICAL REPORT

ARPA Order Number:	2840 Amend. #4
Program Code Number:	6E20
Contractor:	Kansas State University Manhattan, Kansas 66506
Effective date of Contract:	January 1, 1976
Contract Expiration Date:	December 31, 1976
Amount of Contract:	$35,000
Contract Number:	N00014-76-C-0380
Principal Investigator:	D. W. Setser 913-532-6692
Scientific Officer:	Director, Physics Program Physical Science Division Office of Naval Research 800 N. Quincy Street Arlington, VA 22217
Short Title of Work:	Mechanisms, Branching Ratio and Rate Constants in Rare Gas Systems
Sponsored by:	Advanced Research Projects Agency ARPA Order No. 2840/4
Disclaimer:	The views and conclusions contained in this document are those of the authors and should not be interpreted as necessarily representing the official policies, either expressed or implied, of the Advanced Research Projects Agency of the U.S. Government.

ANNUAL TECHNICAL REPORT

(Contract No. N00014-76-C-0380)

MECHANISMS, BRANCHING RATIOS AND RATE CONSTANTS FOR EXCITATION PROCESSES IN RARE GAS SYSTEMS.

Summary

The work done with support from this contract can be divided into three categories:

I. Measurement of total quenching rate constants and branching fractions for krypton halide formation for metastable krypton atoms reacting with halogen containing molecules. These results can be compared to similar data obtained previously from this laboratory for reactions of argon and xenon metastable atoms. The decay of $Kr(^3P_2)$ and $Xe(^3P_2)$ in pure argon also has been studied.

II. Construction of an apparatus which will permit the measurement of the rate constants for electronic excitation of products from charge transfer reactions of He_2^+. These charge transfer reactions will be compared to the Penning ionization reactions of $He(2^3S)$ atoms; some data have been acquired for the latter and are included here.

III. Investigation of the applicability of the ionic-covalent curve-crossing mechanism for the formation of Br_2^*, I_2^* and other excited states of molecular halogens that have been demonstrated to be candidates for U.V. lasers.

All of this work is directed towards discovery of new excitation processes in electrically pumped rare gases that might lead to new visible and U.V. lasers or to measurement of kinetic data that will be of value to modeling calculations for known laser systems.

Dr. Robert Chang and Mr. John Kolts worked full time on the contract. In spite of this being the first year of effort, a reasonable amount of laboratory measurements have been made. This report will be divided into three chapters according to the topics outlined above. A paper has been published describing the work done in III, and the reprint of that paper comprises the section for III. The report for the other two sections has been written in a style that

will permit expansion into manuscripts suitable for journal publication; experimental data rather than extensive interpretation are emphasized. In addition to the data obtained for $He(2^3S)$ reactions, construction of the apparatus that will be used to monitor He_2^+ reactions is described in Section II.

I. Diffusion, Two-Body, and Three-Body Deactivation for $Ar(^3P_2)$, $Ar(^3P_0)$, $Kr(^3P_2)$ and $Xe(^3P_2)$ in Argon and Total Quenching Rate Constants for $Kr(^3P_2)$ with Various Molecules.

J. H. Kolts and D. W. Setser

I-A. Introduction

Interest has focused on electronic energy transfer reactions of the rare gas metastable states, because this class of reactions is of considerable importance to visible and ultraviolet lasers. In previous work from this laboratory, the total quenching rate constants have been reported for the reactions of $Ar(^3P_2)$, $Ar(^3P_0)$, $Xe(^3P_2)$, and to much lesser extent for $Kr(^3P_2)$ with various quenching molecules.[1,2,3] These experimental measurements have employed the flowing afterglow technique. As will be demonstrated by the data reported here, the total quenching rate constants for $Kr(^3P_2)$ generally follow the trend established for $Ar(^3P_2)$ and $Xe(^3P_2)$ metastable states. By combining the total quenching rate constants, k_Q, with the rate constants for individual exit channels, k_{qi}; the branching fraction k_{qi}/k_Q for individual exit channels can be ascertained. The determination of the exit channel rate constants by emission spectroscopy, will be the objective of our future work.

In addition to rate constants for quenching by additive molecules, preliminary rate constants for the diffusion, two-body deactivation, and three-body deactivation rates or $Ar(^3P_2)$, $Ar(^3P_0)$, $Kr(^3P_2)$ and $Xe(^3P_2)$ in <u>argon</u> have been obtained. Results for $Ar(^3P_2)$ and $Ar(^3P_0)$, which can be compared with literature values, support the validity of the experimental technique. The two-body rate constant for $Ar(^3P_0)$ is approximately ten-fold larger than for $Ar(^3P_2)$; however, the three-body rate constants are about equal. The two-body rate constants for $Kr(^3P_2)$ and $Xe(^3P_2)$ resemble that for $Ar(^3P_2)$. The three-body rate constant for $Kr(^3P_2)$ is a factor of 3 lower than for $Ar(^3P_2)$; the three-body rate constant for $Xe(^3P_2)$ was too small to be experimentally measured.

I-B. Experimental Results

The experimental flowing afterglow apparatus was essentially that used in previous work.[1,2,3] Argon metastables were produced in a cold-cathode discharge; the gas flow subsequently passes through a right angle bend to

eliminate effects arising from trapping of resonant radiation produced in the cold-cathode discharge. Krypton and xenon metastables were produced by adding either krypton or xenon to the gas flow upstream of the discharge. Enough xenon or krypton is added to eliminate all of the argon metastable atoms before the gas flow reaches the reaction region. Typical xenon and krypton flows are 0.10 mmole/min and 0.60 mmoles/min, respectively. The Ar carrier flow is 0.152 moles/min.

The reactor portion of the flow tube consists of 31 mm i.d. pyrex tube fitted with a shower head reagent inlet system and quartz observation windows spaced along the flow tube. Typical flow velocities are 80 to 90 meters per second; the pumping was provided by a Roots type blower backed by a 50 1/sec mechanical pump. Flow tube pressures were monitored using a Celesco Industries PD7 pressure transducer, positioned at the midpoint of the flow reactor. Argon flows were measured using a Fischer-Porter floating-ball flow meter.

The concentration of Ar, Kr, or Xe metastables was followed by atomic absorption spectroscopy using a modified Beer-Lambert law,[1]

$$I = I_o[\exp-a([M^*]1)^{\gamma}], \qquad (1)$$

with $\gamma = 0.95$ and [M*] being the metastable atom in question. Source lamps used for the absorption measurements were Oriel Optics pen-ray lamps operated in the AC mode. The optical system consisted of a 0.3m McPherson monochromator fitted with a RCA 7102 photomultiplier tube cooled to approximately 240°K. The light beam was chopped and fed to a PAR phase-lock amplifier. The absorption of the Kr 811.2 nm line was typically 23% for a triple light pass across the reactor. This absorption corresponds to a metastable krypton atom concentration in the flow reactor of $\sim 1 \times 10^{10}$ metastables cm^{-3}. The concentrations of $Xe(^3P_2)$ and $Ar(^3P_2)$ are higher by a factor of ~ 2.

Argon carrier gas was supplied by Air Products with a rated purity of 99.995%. Prior to entering the discharge, the argon was first passed at high pressure through a room temperature zeolite trap and then through two low pressure liquid nitrogen cooled zeolite traps. Krypton and xenon was purchased from Cryogenic Rare Gas Labs (Research Grade) and were metered into the Ar flow without further purification. Reagents used for the determination of total quenching rate constants were either distilled or sublimed under vacuum several times before being mixed with argon diluent (85 to 90%). Most reagents were stored in glass storage bulbs. Florine and flourine containing reagents, which react with glass, were stored in passivated stainless steel containers. Reagent flows, typically 1-20 μmoles/min, were measured by monitoring the change in pressure-vs-time in a calibrated standard volume. Without altering

the flow, the reagent gas then was diverted to the flow reactor for the quenching measurements.

To find D_o, k_1, k_2 and k_Q the following first order rate law was used:

$$\ln \frac{[M^*]}{[M^*]} = -\left(\frac{D_o}{\Lambda^2[Ar]} + k_1[Ar] + k_2[Ar]^2 + k_Q[Q]\right)t. \qquad (2)$$

D_o is the diffusion coefficient, Λ is the characteristic diffusion length, k_1 is the two-body deactivation rate constant, k_2 is the three-body deactivation rate constant, and k_Q is the quenching rate constant for the reagent, Q. For low values of absorption, $\leq$25%, the Beer-Lambert relation can be used and $\ln(\ln I/I_o) \alpha \ln[M^*]/[M^*]o$. The concentration of the $Kr(^3P_1)$ and $Kr(^3P_0)$ states were below the detectable limits of atomic absorption spectroscopy. Thus, these states can not affect the kinetics for $Kr(^3P_2)$. Also the concentration of Kr is sufficiently small that encounters between $Kr(^3P_2)$ and Kr can be neglected.

In the absence of added reagent, the pseudo first order rate constant, K' governing the decay of the metastable atoms is given by

$$K' = \frac{D_o}{\Lambda^2[Ar]} + k_1[Ar] + k_2[Ar]^2. \qquad (3)$$

The pseudo first order rate constants are measured by observing the decay of [M*] along the flow reactor. The results for $Kr(^3P_2)$ and shown in Figure 1 for the 0.5 to 3.5 torr range. In order to assign D_o, k_1 and k_2, these K' values were fitted to equation 3 using a non-linear least-squares computer routine. The line in Figure 1 shows the degree of fit. The range of pressure that can be used is rather narrow because as K' increases, [M*] rapidly declines at the last few windows. A further limitation is that the Roots blower can accept only 3 Torr at the entrance port without overheating. In order to obtain higher pressure, it is necessary to throttle the flow, which further accelerates the decay of [M*] along the tubular reactor. Additional measurements are needed at higher pressure to permit more reliable rate constant assignments; however, preliminary values of the rate constants are reported in Table I along with some pertinent literature values. The diffusion coefficient and two-body de-excitation rate constants for $Ar(^3P_0)$ compare well with the results of Ellis and Twiddy; however, the three-body deactivation is a factor of two larger than their value. In the case of $Ar(^3P_2)$, our two-body rate constant agrees with the literature values but again the three-body rate constant is larger than the generally accepted value. We are unaware of any prior measurement of the decay constants for

FIGURE 1

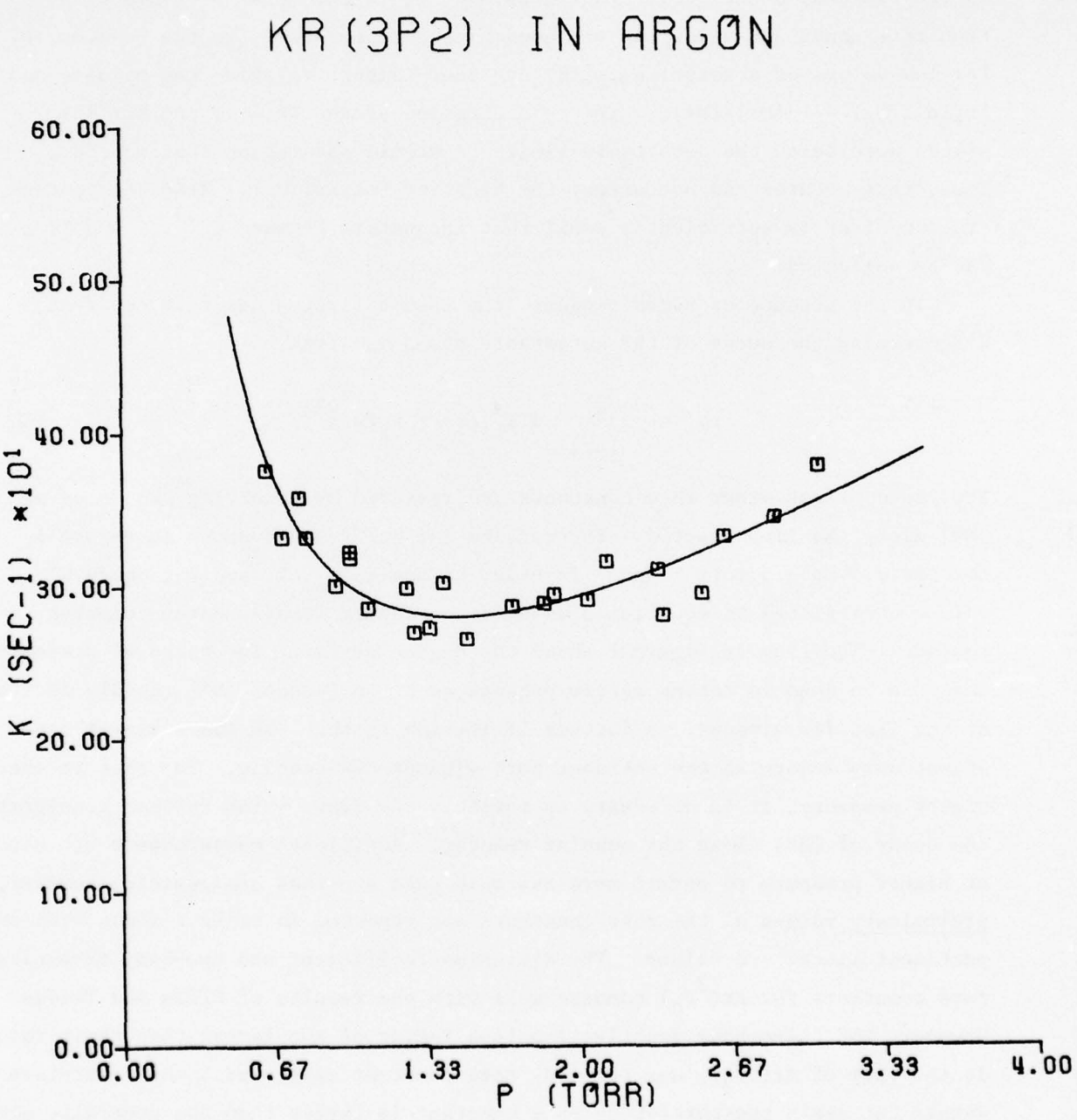
KR(3P2) IN ARGON
60.00
50.00
40.00
30.00
20.00
10.00
0.00
K (SEC-1) *10^1
0.00
0.67
1.33
2.00
2.67
3.33
4.00
P (TORR)

Table I Diffusion, Two-Body, and Three-Body Rate Constants

System	Do($cm^{-1}sec^{-1}$)	k_1($cm^3molec^{-1}sec^{-1}$)	k_2($cm^6molec^{-2}sec^{-1}$)
$Ar(^3P_0)+Ar$	$(1.98\pm0.1)\times10^{18}$[a]	$(5.22\pm0.9)\times10^{-15}$[a]	$(2.6\pm0.9)\times10^{-32}$[a]
	$(1.77\pm0.17)\times10^{18}$[b]	$(5.6\pm0.7)\times10^{-15}$[b]	$(1.4\pm0.15)\times10^{-32}$[b]
$Ar(^3P_2)+Ar$	$(2.09\pm0.1)\times10^{18}$[a]	$(0.75\pm0.3)\times10^{15}$[a]	$(3.34\pm0.4)\times10^{-32}$[a]
	$(1.66\pm0.17)\times10^{18}$[b]	$(1.0\pm0.3)\times10^{-15}$[b]	$(1.7\pm0.2)\times10^{-32}$[b]
	1.76×10^{18}[c]	1.23×10^{-15}[c]	0.85×10^{-32}[c]
$Kr(^3P_2)+Ar$	$(3.22\pm0.3)\times10^{18}$[a]	$(1.69\pm0.6)\times10^{-15}$[a]	$(1.25\pm0.7)\times10^{-32}$[a]
$Xe(^3P_2)+Ar$	$(3.14\pm0.4)\times10^{18}$[a]	$(1.73\pm0.6)\times10^{-15}$[a]	$(0.1\pm0.1)\times10^{-32}$[a]
$Kr(^3P_2)+Kr$	1.52×10^{18}[d]	9.0×10^{-15}[d]	5.36×10^{-32}[d]
	0.91×10^{18}[e]	2.44×10^{-15}[e]	2.59×10^{-32}[e]
$Xe(^3P_2)+Xe$		3.65×10^{-15}[f]	8.5×10^{-32}[f]

a. This work

b. E. Ellis and N. D. Twiddy, J. Phys.,B: Atom Molec. Phys. 2, 1366 (1969)

c. A. V. Phelps and J. P. Molnar, Phys. Rev. 89, 1202 (1953)

d. R. T. Ku, J. T. Verdeyen, B. E. Cherrington, and J. G. Eden, Phys. Rev. A8, 3123 (1973)

e. C. J. Tracy and H. J. Oskam, J. Chem. Phys., 65, 1666, (1976)

f. P. R. Timpson and J. M. Anderson, Can. J. Phys. 48, 1817 (1970)

$Kr(^3P_2)$ and $Xe(^3P_2)$ in Ar. The values of $Kr(^3P_2)$ in krypton and $Xe(^3P_2)$ in xenon are included in Table I for comparison purposes. In each case the two-body rate constants in Ar much smaller than in the heavier rare gas. In fact the two-body rate constants for $Ar(^3P_2)$, $Kr(^3P_2)$ and $Xe(^3P_2)$ are the same to within experimental error. The most interesting finding is that the three-body rate constant for $Kr(^3P_2)$ in Ar is "normal"; whereas, for $Xe(^3P_2)$ the three-body rate constant was too low to be measured (note that the error limit gives an upper limit of $<0.2 \times 10^{-32}$ cm^6 $molec^{-1}$ sec^{-1}).

For the determination of the quenching rate constants by added reagent, the [M] is measured vs distance for a fixed concentration of [Q] and constant argon pressure. The experiment is repeated for various flows of reagent (see figure 2) and a set of pseudo first order rate constants for various Q are obtained. Then rate constants are plotted vs Q, see Figure 3, and the slope from the resulting line gives the quenching rate constants for various Q. Actual data reduction is done using linear least square fits; typical standard deviation are $\pm$10%. The absolute uncertainty is considerably larger because of uncertainties in the conversion of flow distance to flow times. The long-term reproducibility was checked by studying the reactions of $Kr(^3P_2) + NF_3$ and $Xe(^3P_2) + Br_2$. Three separate experiments were done for each case using three different mixtures with time periods between experiments of up to eight months. For each case the deviation from reported values was less than 10%. As a check on our handling procedures of florine compounds, separate runs were made on a laboratory prepared F_2 mixture and a commercially prepared F_2 mixture. Rate constant values for $Kr(^3P_2) + F_2$ for the two mixtures were 61 and 71 $\times 10^{-11}$ cm^3 $molec^{-1}$ sec^{-1}, respectively.

The work done during the past year has been focused upon $Kr(^3P_2)$ reactions. The results are tabulated in Table 2; previous studies with $Ar(^3P_2)$ and $Xe(^3P_2)$ are included for sake of completeness. With the exception of some of the reagents which have small rate constants, the values of k_Q for the same reagent tend to be similar for all three metastable atoms. Three noteable exceptions may be C_2H_6, N_2O and CO_2 reacting with $Kr(^3P_2)$; these molecules will be reinvestigated to further check the values in Table 2. Conversion of the rate constants to cross-sections give cross-section values that do increase somewhat in the Ar, Kr, Xe series, because the thermal velocity declines in the series, i.e. $\sigma_Q = k_Q/\langle v \rangle$. The rate constant measurements are nearly complete. We only

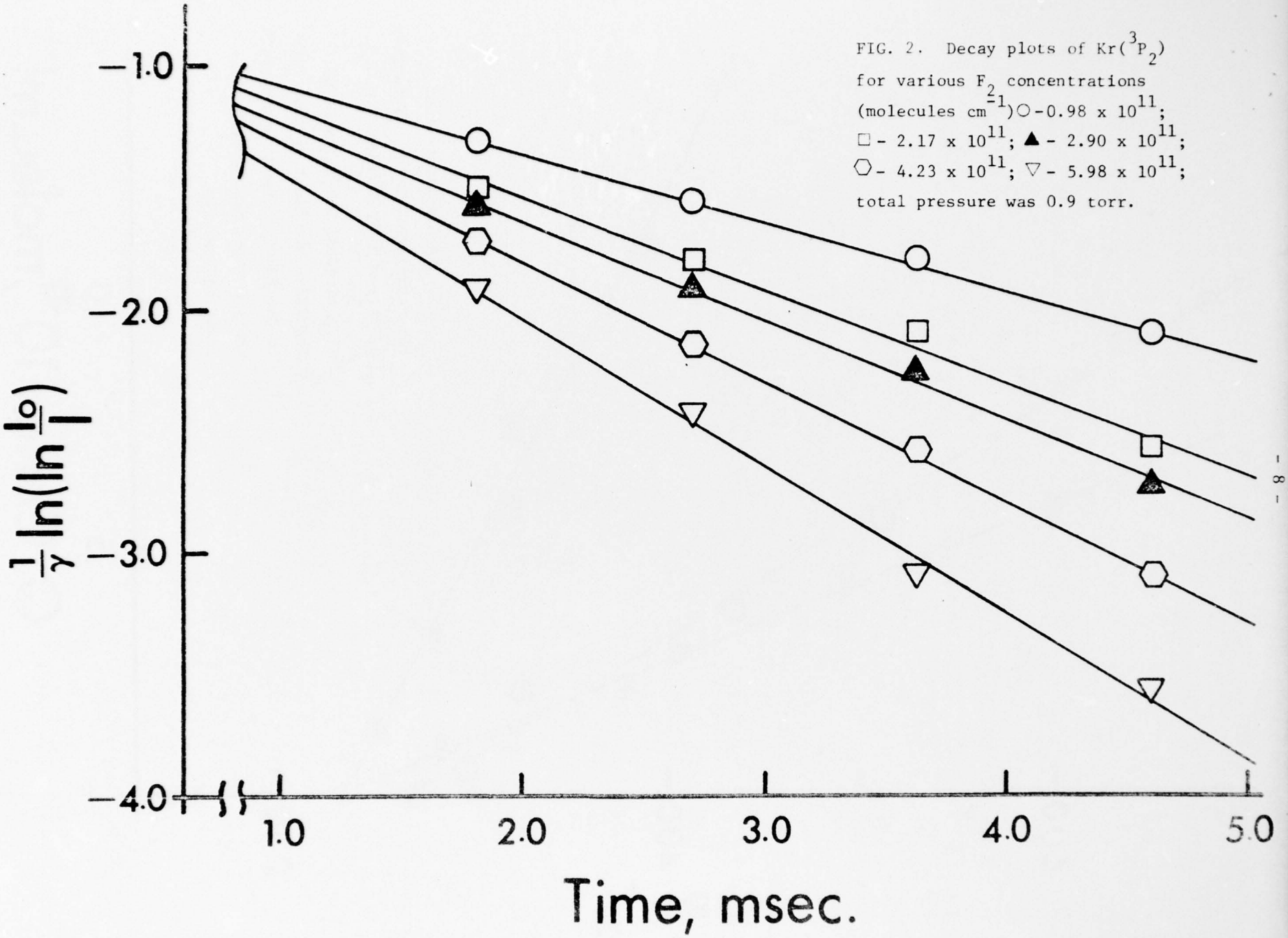

FIG. 2. Decay plots of $Kr(^3P_2)$ for various F_2 concentrations (molecules cm^{-1}) ○ - 0.98×10^{11}; □ - 2.17×10^{11}; ▲ - 2.90×10^{11}; ⬡ - 4.23×10^{11}; ▽ - 5.98×10^{11}; total pressure was 0.9 torr.

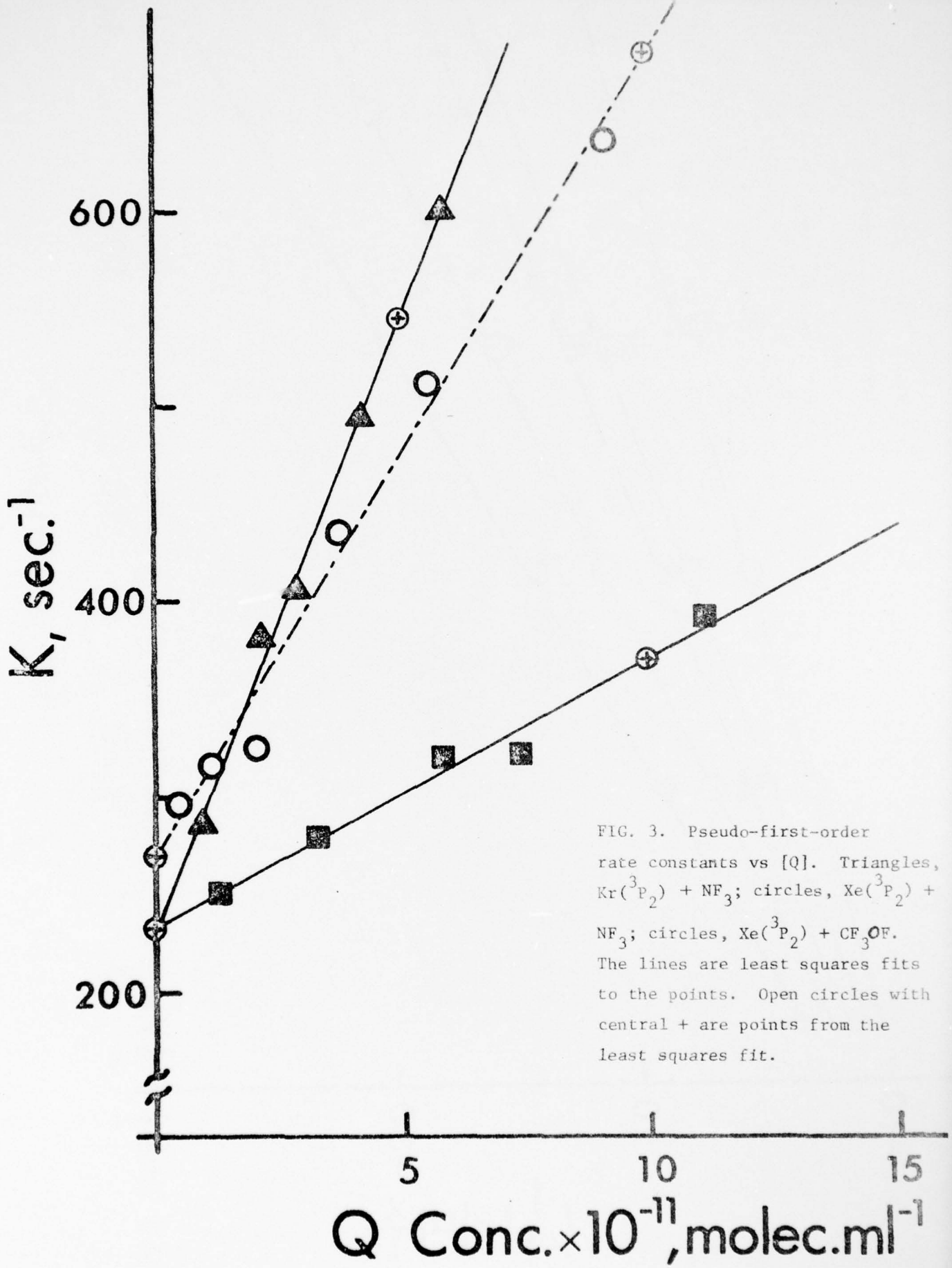

FIG. 3. Pseudo-first-order rate constants vs [Q]. Triangles, $Kr(^3P_2) + NF_3$; circles, $Xe(^3P_2) + NF_3$; circles, $Xe(^3P_2) + CF_3OF$. The lines are least squares fits to the points. Open circles with central + are points from the least squares fit.

Table 2 Quenching Rate Constants (10^{-11} cm^3 $molec^{-1}$ sec^{-1})

Reagent	$Ar(^3P_2)$		$Kr(^3P_2)$		$Xe(^3P_2)$	
	k_Q	$\sigma(Å^2)$[a]	k_Q	$\sigma(Å^2)$[a]	k_Q	$\sigma(Å^2)$[a]
F_2	75	132	72	146	75	161
Cl_2	71	142	73	179	72	193
Br_2	65	147	61	178	60	202
ICl	61	138	48	143	50	171
IBr			70	216		
ClF	74	141	68	156	63	154
OF_2	57	107	53	121	57	139
NOCl	48	95			51	139
NOF	36	68	47	102	45	106
NF_3	14	28	12	29	8	23
N_2F_4	31	65	33	90		
CF_3OF	42	90	42	114	47	143
SF_6	16	36	18	51	23	75
SeF_6	71	166			65	246
TeF_6	58	135			63	230
SO_2F_2	42	89				
S_2Cl_2	53	115	48	129	49	150
$SOCl_2$	67	145	58	163	58	182
CF_4	4	8	0.07	0.2	<0.03	0.1
CF_3H	31	64	15	37	0.2	0.6
CF_2H_2			35	79	40.9	99
CH_3F					44	91
CH_4	33	45	37	54	33	49

Table 2 continued

Reagent	$Ar(^3P_2)$		$Kr(^3P_2)$		$Xe(^3P_2)$	
	k_Q	$\sigma(\AA^2)$	k_Q	$\sigma(\AA^2)$	k_Q	$\sigma(\AA^2)$
C_2H_6	66	109	50	93	64	125
N_2	3.6	5.8	0.39	.7	1.9	3.7
N_2O	44	81	31	66	44	100
NO	22	36	16	29	25	48
SO_2			58	139		
O_2	21	35	16	31	22	44
H_2	6.6	3.6	3	1.7	1.6	0.9
CO	1.4	2.3	5.7	10	3.6	7.0
CO_2	53	97	34	72	45	103
Xe	18	40	16	46		
Kr	0.6	1.3				

intend to measure rate constants for Hg, D_2 and a limited number of other reagents. Attention than will be given to determination of products from the quenching reactions.

I-C Discussion of Results

Although the values assigned to the diffusion coefficients, the two-body deactivation rate constants and the three-body deactivation rate constants are preliminary, they are sufficiently reliable to reach some tentative conclusions. The diffusion coefficients for the metastable atoms are all smaller than for ground state atoms because of the increased physical size of the excited state atoms. Although the effect may be magnified by experimental error, the diffusion coefficients for $Xr(^3P_2)$ and $Xe(^3P_2)$ appear to be larger than for $Ar(^3P_2)$; all are in Ar. This can be attributed, at least in part, to the combination of energy exchange and mass diffusion for Ar* in Ar. This combination of processes is known to lower the apparent observed diffusion coefficient.[5]

The physical interpretation of the two-body deactivation process for the $(^3P_2)$ states is not well established. Collisional excitation to the $^3P_1$ level, followed by subsequent rapid decay, is not consistent with the nearly equal magnitudes of the rate constants found for $Ar(^3P_2)$, $Kr(^3P_2)$ and $Xe(^3P_2)$ in argon because the energy separation between the $^3P_1$ and $^3P_2$ states increases in the series; 607, 945, and 977 cm^{-1}. This conclusion is supported by the lack of a temperature coefficient for the two-body step.[7] Thus, the two-body term may be collision induced radiation (or radiative recombination). Another alternative is the following set of processes, written for convenience for $Ar(^3P_2)$.

$$Ar(^3P_2) + 2Ar \xrightarrow{k_A} Ar_2^{**} + Ar$$

$$Ar_2^{**} \xrightarrow{k_B} h\upsilon + 2Ar$$

$$+ Ar \xrightarrow{k_C} Ar(^3P_2) + 2Ar$$

The steady state expression gives $[Ar_2^{**}] = k_A[Ar(^3P_2)][Ar_2]^2/(k_B + k_C[Ar])$. The loss rate of $Ar[^3P_2]$ is given by

$$k_B[Ar_2^{**}] = \frac{k_B k_A[Ar(^3P_2)][Ar_2]^2}{k_B + k_C[Ar]}$$

and if $k_C[Ar] > k_B$ then an effective two-body decay process results. The Ar_2^{**} is used to represent bound states just slightly below the dissociation

limit. A scheme similar to that above has been invoked to explain the collision induced emission from $O(^1S)$ by rare gases.[8] More work clearly remains to be done to characterize these two-body processes.

The most interesting result, as well as the most pertinent for laser systems, is the slow three-body process for $Xe(^3P_2)$ in argon. Since the three-body process represents diatomic excimer formation, this result is consistent with the failure to observe[9,10] emission from an ArXe* excimer in Ar/Xe mixtures excited by discharge or absorption of vac U.V. resonance energy. The ArXe* excimer must have a very small binding energy. In contrast the ArKr* excimer emission has been observed[9,10], which is consistent with a "normal" three-body rate constant. During the next few months, we hope to study the vacuum U.V. emissions from $Ar(^3P_2)$, $Xe(^3P_2)$ and $Kr(^3P_2)$ in argon using the discharge flow apparatus. Such observations should help to characterize the final product states from the three-body and two-body steps.

Discussion of the $Kr(^3P_2)$ quenching rate constants will be delayed until more is known about the exit channel distributions. At the present time KrF* formation rate constants from F_2, NF_3, N_2F_4, OF_2, CF_3OF, NOF and ClF have been investigated. The results are tabulated in Reference 3. The branching fraction for KrF formation was unity only for F_2 and OF_2. In general the branching fractions for XeF* formation tend to be higher than for KrF* formation. A special study[11] has been done with XeF_2*. In this case, excitation transfer giving XeF_2^*, which subsequently predissociates to give XeF*, competes with reactive quenching giving KrF* + Xe + F. The KrF* emission (at low pressure) extends from 2450 Å to slightly beyond 1950 Å. The emission from the other krypton halides occur at even shorter wavelengths. Thus, vacuum U.V. observations are necessary to definitely measure the exit channel rate constants. In doing this work, we intend to use the internal standard method[3] with either Cl_2 or F_2 serving as the standard.

I-D References

1. L. G. Piper, J. E. Valazco, and D. W. Setser, J. Chem. Phys., 59, 3323 (1973).
2. J. E. Velazco and D. W. Setser, Chem. Phys. Lett., 25, 197 (1974).
3. J. E. Velazco, J. H. Kolts and D. W. Setser, J. Chem. Phys., 65, 3468 (1976).
4. C. J. Tracy and H. J. Oskam, J. Chem. Phys. 65, 1666 (1976).
5. G. Fujimoto, A. Nitzen and E. Weitz, Chem. Phys. 15, 217 (1976).
6. D. L. King and D. W. Setser, Ann. Rev. Phys. Chem. 27, 407 (1976).
7. A. H. Futch and F. A. Grant, Phys. Rev. 104, 356 (1956).
8. G. Black, R. L. Sharpless, T. Slanger, J. Chem. Phys. 63, 4546 (1975).
9. O. Chesnovsky, A. Gedanken, B. Raz and J. Jortner, Chem. Phys. Lett. 22, 23 (1973).
10. O. Chesnovsky, B. Raz and J. Jortner, J. Chem. Phys. 57, 4625 (1973).
11. J. E. Velazco, J. H. Kolts and D. W. Setser, Chem. Phys. Lett. In Press (1977).

II-A Construction of a Flowing Afterglow Apparatus for the study of He_2^+ Reactions

The construction of a new flowing afterglow apparatus that can generate and monitor He_2^+, as well as observe the emission from electronically excited products generated by charge transfer reactions with He_2^+, is the major construction project of this contract. The block diagram below summarizes the components of the apparatus.

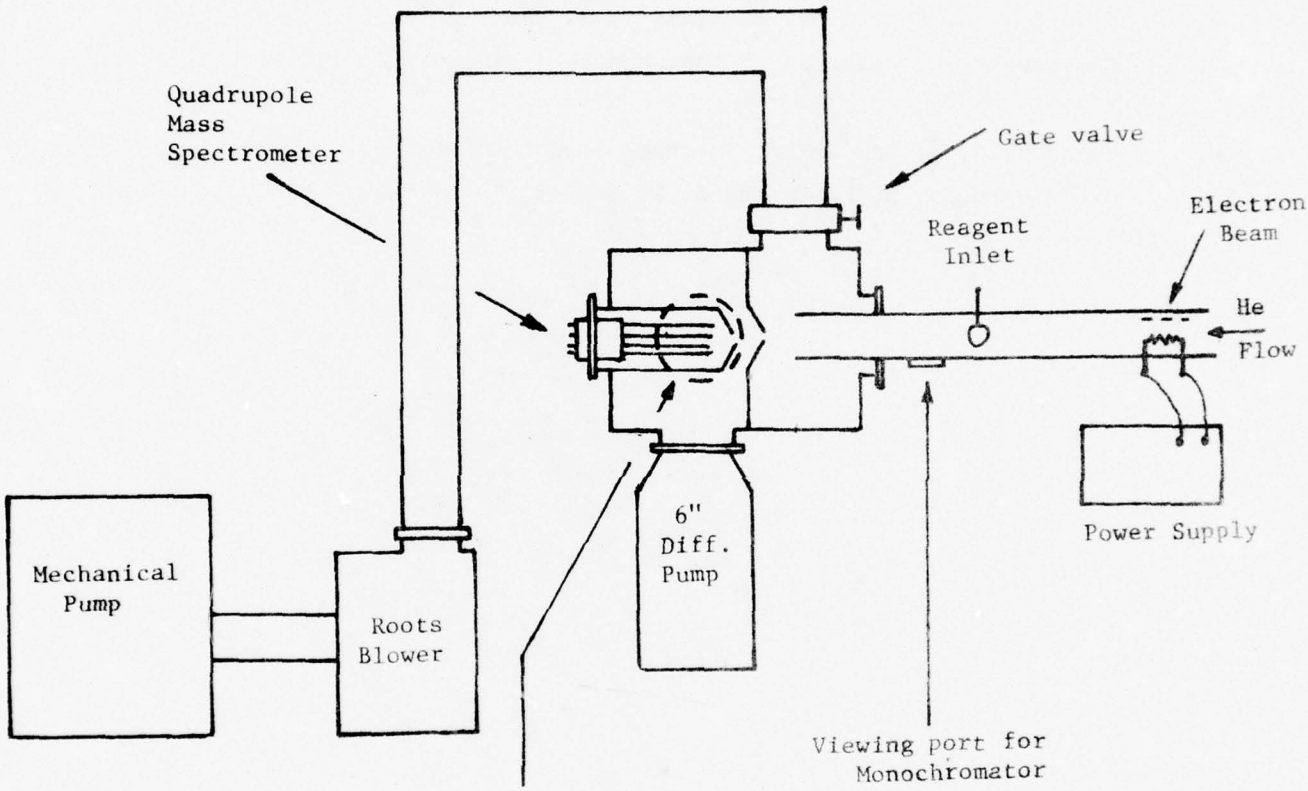

The 4" pumping part is denoted by the dotted lines. It is used to pump the 4" pipe behind the second pinhole.

All of the equipment needed for the spectroscopic measurements are readily available in our laboratory. The quadrupole mass spectrometer and the 4" and 6" pumping stations also were available. However, it was necessary to purchase the large mechanical pump, the Roots blower, materials for the differential sampling inlet for the mass spectrometer, components for the flow tube, and all gas handling and pressure measuring components. The pumping system has been designed so that high pressures (~10 torr) can be accepted by the blower. This is important since He_2^+ is generated by the three-body recombinations of He^+ ions. As of January 1, 1977, all of the apparatus shown in the diagram, except the electron gun filaments and power supply, were installed. However, considerable work remains to be done before experiments can be done. The most important tasks are tuning up the mass spectrometer, which has not been used for about 18 months, reduction of vibrations from the large pump, adjustment of the sizes of the pinhole leaks on the nose cones separating the differential pumping zones, and developing the "proper" bias potentials on the nose cones for sampling of positive ions. We are in close contact with Dr. Dan Albritton of the NOAA labs and will be following his advice with respect to solving these as well as problems that may develop. This work is being done by Mr. John Kolts. During the first year, he has mainly supervised the shop personnel in construction of the sampling interface and assembled components as they become available. John's main laboratory efforts have been on measuring the metastable $Kr(^3P_2)$ reaction kinetics (see section I). During the forthcoming year, John will divide his time between completing the $Kr(^3P_2)$ measurements and bringing the new He_2^+ flowing afterglow apparatus into operation.

II-B Rate Constants for Exit Channels Giving Emission from Quenching of $He(2^3S)$ by Small Molecules.

R. S. F. Chang and D. W. Setser

Introduction

The total quenching rate constants for metastable[1-4] and resonance[5] states of the rare gas atoms have been measured for a variety of reagents. For quenching of the metastable atoms by efficient molecular reagents, a correlation

has been found between the magnitude of the quenching cross-sections and the C_6 coefficient[1] or polarizability[2] of the reagent molecule. This correlation is evidence that the magnitude of the quenching cross-section is determined by long range interactions in the entrance channel. However, the distribution of exit channels is determined by subsequent shorter range interactions during the collision process. In order to more fully understand the quenching reactions, the exit channels need to be characterized. Our laboratory has recently assigned some product distributions from the quenching of the heavy metastable rare gas atoms.[1] The present work is a continuation of our efforts and deals mainly with product distributions from quenching by $He(2^3S)$. Although the available energy from $He(2^3S)$, 19.80 eV, exceeds the ionization potential, neutral dissociation can be an important exit channel rather than Penning ionization.[6] In this work reference reactions with known rate constants for a given emission are used to assign the rate constants for dissociative excitation of hydrocarbons and Penning ionization of small molecules. The reactions of N_2 or CO with $He(2^3S)$ yielding $N_2^+(B)$ and $CO^+(B)$ are shown to be suitable reference reactions for emissions excited by metastable helium atom reactions.

Experimental

The cold hollow-cathode discharge source and the flow tube used in this study were similar to the designs previously utilized for observation of emissions from reaction of metastable rare gas atoms.[1] All observations were made at a pressure of 2 torr or less to exclude excitation from sources other than the metastable atoms, i.e., atomic and molecular ions of helium. The concentration of the metastable atoms were in the 10^{10} -10^{11} cm^{-3} range. Reagent gases were mixed with helium and stored in reservoirs. For most of the measurements, mixtures of the reagent and reference molecule (N_2 or CO) were prepared. For these experiments the mole fraction of the components, but not the absolute flow rates, are needed. Spectra were obtained with a 0.75 meter Jarrell-Ash monochromator fitted with EMI 9558Q photomultiplier tube and SSR photon counting rate meter. Data from this monochromator were taken with computer control of the monochromator drive. The response of this detection system was calibrated from 190-850 nm. Correction for the response was done via the computer as the emission intensities were integrated.

Reference Reactions for Assignment of Dissociative Excitation Rate Constants.

The rate constant for an observed emission process can be easily assigned

by comparison to the intensity from a reaction channel with a known rate constant. In this section the N_2 and CO reactions with $He(2^3S)$ will be shown to be suitable reference reactions for $He(2^3S)$. The total quenching rate constants for CO and N_2 have been measured several times[4] using the flowing afterglow technique. The branching ratios for the various products have been ascertained from energy analysis fo the electrons[9,13] and from observation of emission intensities.[6,14] These are listed in Table 1. To assign the formation rate constants for the various channels in Table 2, we used the total rate constants of Ref. 4a and the branching ratios of Ref. 6a and 13 as being most representative of the available data.

Experiments were done to confirm the expected ratio of formation rate constants for $N_2^+(B-X)$ and $CO^+(B-X)$ by comparing emission intensities for the same concentration of $He(2^3S)$. Assuming there is no quenching of any of the

$$He_2(^3S) + N_2 \rightarrow N_2^+(B) + He + e^-$$
$$+ CO \rightarrow CO^+(B) + He + e^-$$

emitting states, the relative emission intensity from a prepared mixture of N_2 and CO is given by,

$$\frac{I_{CO^+(B-X)}}{I_{N_2^+(B-X)}} = \frac{k_{CO^+(B)}[CO]}{k_{N_2^+(B)}[N_2]} = \frac{\sigma_{CO^+(B)}(\mu_{CO + He^*})^{-1/2}[CO]}{\sigma_{N_2^+(B)}(\mu_{N_2 + He^*})^{-1/2}[N_2]} \qquad (1)$$

where I is the total emission intensity of the (B-X) system of the ionic species; k is the rate constant for producing the ionic species in the B state via $He(2^3S)$ Penning Ionization; σ is the mean thermal excitation cross section; and μ is the reduced mass of the respective $He(2^3S)$ neutral system. Thus, a plot of $I_{CO^+(B-X)}/I_{N_2^+(B-X)}$ versus $[CO]/[N_2]$ will yield a straight line of slope $k_{CO^+(B)}/k_{N_2^+(B)}$. Six prepared mixtures of CO and N_2 diluted in helium with different CO/N_2 ratios were added separately to the helium afterglow at a total pressure of 2 torr. By changing the flow rate of each prepared mixture while maintaining first order condition for the ionic emission intensities, six values of $I_{CO^+(B-X)}/I_{N_2^+(B-X)}$ were determined and averaged to obtain each point on the graph shown in Figure 1. The (0,0) and (1,0) bands of $CO^+(B-X)$ and $N_2^+(B-X)$ emission intensities were measured. Emission from v'>1 were not observed. After correcting for the spectral response of the monochromator/detector these bands were used to scale the observed intensity to the total relative emisssion intensities[15] in the following way;

Table 1. Rate Constants and Product Branching Ratios for $He(2^3S) + N_2$ and CO.

a. Rate constants for the quenching of $He(2^3S)$ at 300°K in units of 10^{-11} cm^3 $molec^{-1}$ sec^{-1}.

N_2	CO	References
6.96	9.85	4a
7.1		4b
6.3		4c
6.7	10.7	4d
10	17	4e
8.6		4f

b. Product branching ratios of the total $He(2^3S) + N_2$ and CO reaction rates.

$N_2^+(B)$	$N_2^+(A)$	$N_2^+(X)$	References
41	24	35	13
41	19	40	9

$CO^+(B)$	$CO^+(A)$	$CO^+(X)$	C^*	References
....	22	51	...	13
27	22	....	...	6a,17
....	22	58	...	9
53	17	26	4	14

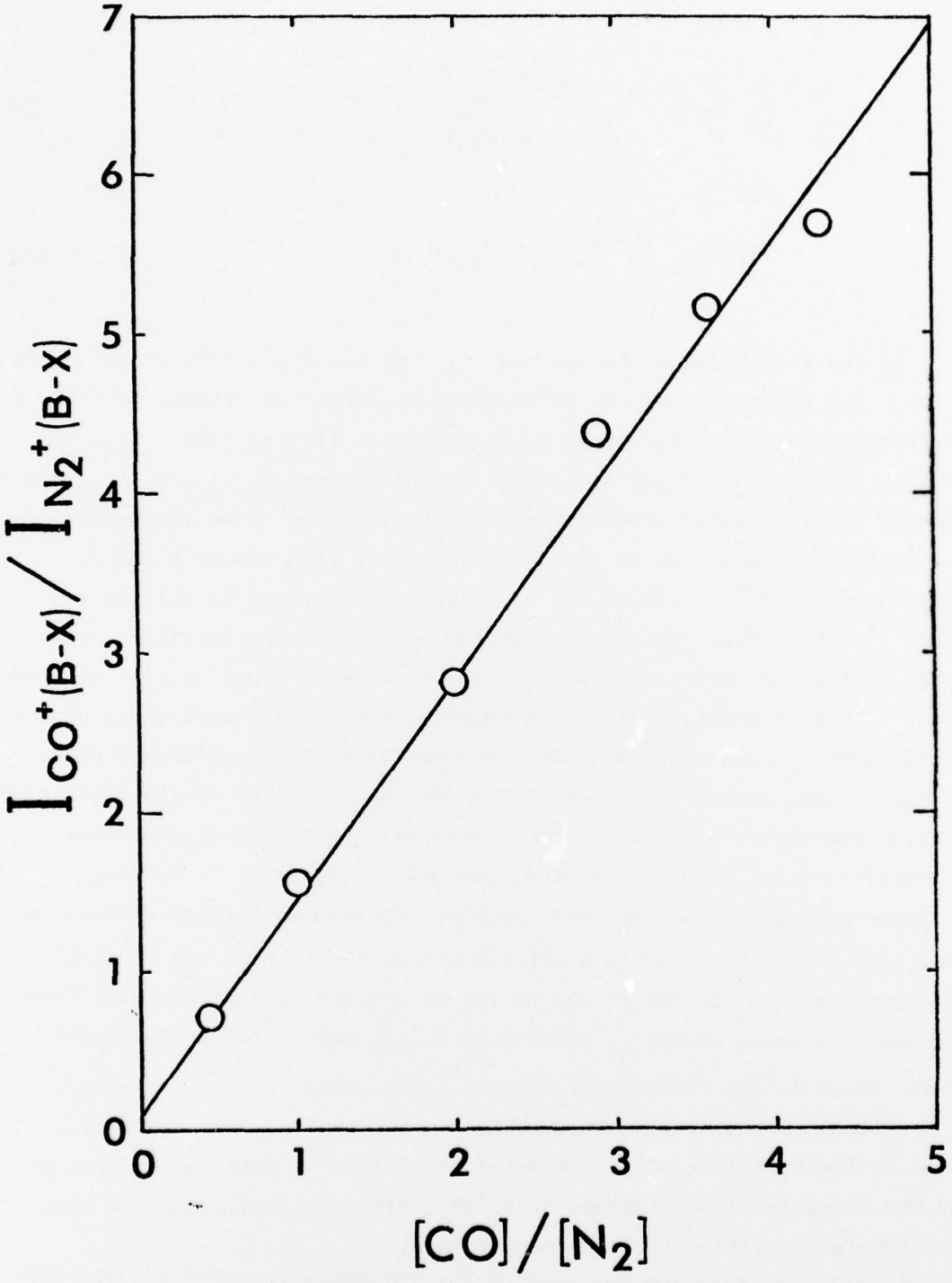

Fig. 1 Plot of $I_{CO^+(B-X)}/I_{N_2^+(B-X)}$ versus $[CO]/[N_2]$. The line is the least squares best fit.

$$\sum_{v''} I_{0,v''} = I_{0,0} \frac{\sum_{v''} q_{0,v''} \nu^3_{0,v''}}{q_{0,0}\nu^3_{0,0}} \quad , \tag{2}$$

$$\sum_{v''} I_{1,v''} = I_{1,0} \frac{\sum_{v''} q_{1,v''} \nu^3_{1,v''}}{q_{1,0}\nu^3_{1,0}} \quad , \tag{3}$$

and

$$I_{TOTAL} = \sum_{v''} (I_{0,v''} + I_{1,v''}) \quad . \tag{4}$$

where $q_{v'v''}$ is the Franck-Condon factor and $\nu_{v'v''}$ is the transition frequency in wave numbers. The scale factors for $CO^+(B-X)$ and $N_2^+(B-X)$ are listed in Table 3. The slope from Figure 1, as determined by least square fit, is 0.68. This can be compared to the ratio obtained from Table 2, which gives $k_{CO^+(B)}/k_{N_2^+(B)} = 0.93$. This agreement is satisfactory considering the large number of measurements from different laboratories involved in obtaining the ratio from Tables 1 and 2.

One advantage of $N_2^+(B)$ and $CO^+(B)$ as reference reactions is that only a small number of vibrational levels are produced by the Penning ionization reaction. Furthermore, most of the emission from a given vibrational level is concentrated in one band. The experimentally measured relative vibrational band areas of the B-X transitions are in good agreement with values calculated from Franck-Condon factors. The present data may suggest a mild dependence of the $CO^+(B)$ transition probabilities upon the r-centroid; however, this will not be discussed here. The relative vibrational populations of $N_2^+(B)$ and $CO^+(B)$ from the Penning reaction are in good agreement with earlier work and need no further discussion. One disadvantage of $He(2^3S)$ + CO as a reference reaction is that the $CO^+(A-X)$ emission is extensive in the 300 to 635 nm region and may overlap emission from the other reactions being studied. Since both $N_2^+(B)$ and $CO^+(B)$ are produced from He_2^+ and since $N_2^+(B)$ is produced from He^+, care must be taken to adjust operating conditions (pressure) so that these ion species make no significant contribution to the $N_2^+(B)$ or $CO^+(B)$ emission intensity.[17] This can be done by monitoring the vibrational populations of $N_2^+(B)$, since the appearance of high vibrational levels identifies the presence of ions.

Since the He* + CO reaction was used as the reference reaction to determine the absolute cross-sections for emission of radiation as a result of Penning

Table 2. Formation rate constants for the products of $He(2^3S) + N_2$ and CO reactions.

Product	Rate Constant (in units of 10^{-11} $cm^3 molec^{-1} sec^{-1}$)
$N_2^+(B)$	2.85
$N_2^+(A)$	1.50
$N_2^+(X)$	2.61
Total	6.96
$CO^+(B)$	2.66
$CO^+(A)$	2.07
$CO^+(X)$	5.12
Total	9.85

Table 3. Scaling Factors for the $N_2^+(B-X)$ and $CO^+(B-X)$ Transitions

	$CO^+(B-X)$[a]	$N_2^+(B-X)$[b]
$\frac{\sum_{v''} q_{0,v''} \nu^3_{0,v''}}{q_{0,0} \nu^3_{0,0}}$	1.69	1.45
$\frac{\sum_{v''} q_{1v''} \nu^3_{1,v''}}{q_{1,0} \nu^3_{1,0}}$	2.52	3.66

a. J. E. Hesser, J. Chem. Phys., 48, 2518 (1968).

b. F. J. Comes and F. Speier, Chem. Phys. Letters, 4, 13 (1969).

ionization for all the molecules studied here, the accuracy of the excitation cross-section of $CO^+(B)$ itself becomes crucial. Hurt and Grable[14] have reported a $CO^+(B)/CO^+(A)$ ratio of 3.1:1.0 from Penning ionization, a value quite different from the ratio 1.23:1.0 determined in this laboratory using the same experimental technique. If the total $He(2^3S)$ quenching cross-section for CO were partitioned according to Hurt and Grable's results, the ratio of $\sigma_{CO^+(B)}$ to $\sigma_{N_2^+(B)}$ would be 2.15, which is more than three times larger than the experimental value measured here.

Results

He* + Hydrocarbons

Neutral dissociative excitation pathways for the quenching of $He(2^3S)$ by the simplest members of the aliphatic, cyclane, aromatic, olefinic and acetylenic hydrocarbon series were studied. Table 4 summarizes the spectra observed from each reaction. Experiments also were done in the vacuum ultraviolet region; however, only H Lyman-α emission was observed. No evidence for ion-electron recombination reactions as an excitation pathway was found for any of these systems. The dissociative excitation cross-sections for quenching of $He(2^3S)$ by the hydrocarbons was measured by comparing the emission intensities of either $CO^+(B)$ or $N_2^+(B)$ to the total emission intensity from the hydrocarbons, i.e.

$$\frac{I_{CO^+(B-X)}}{I_{HC}} = \frac{k_{CO^+(B)}[CO]}{k^*_{HC}[HC]} \approx \frac{\langle\sigma_{CO^+(B)}\rangle(\mu_{CO-He^*})^{-1/2}[CO]}{\langle\sigma^*_{HC}\rangle(\mu_{HC-He^*})^{-1/2}[HC]} . \qquad (5)$$

The easiest way to do the measurements is to compare intensities from prepared mixtures since this method insures that both reagents are subject to the same $[He(2^3S)]$. If overlap of the emission from HC and $N_2^+(B)$ or $CO^+(B)$ prevents utilization of mixtures, then the emission intensity from HC and $N_2^+(B)$ was obtained separately under conditions (low flows) such that the intensity was first order in reagent. These intensities, corrected for reagent flow, were then compared to obtain rate constants. The total emission intensity from the hydrocarbons was obtained by monitoring the CH(A-X) band system and scaling to the total emission intensity, according to Table 4. The dissociative excitation cross-sections were deduced from the slopes of $I_{HC}/I_{CO^+(B-X)}$ versus [HC]/[CO]

Table 4 - Relative Intensities[a] of Observed Spectra

Reaction	CH(A→X)	CH(B→X)	CH(C→X)	C_2(e-b)	C_2(d-x)	C_2(c-b)[b]	C_2(B→X)	C_2(A-X)	CH^+(B→Σ)	molecular or unassigned[c]	H-lines	CH/C_2[d]
He^* + CH_4	0.67	0.28	0.05	-	-	-	-	-	-	-	<0.01	∞
+ C_2H_4	0.46	0.11	0.04	<<0.01	<0.01	0.02	0.05	0.28	-	~0.02	~0.02	1.63
+ C_2H_2	0.32	0.06	<<0.01	<0.01	0.01	0.07	0.07	0.33	0.03	0.08	<0.01	0.79
+ C_6H_6[f]	0.06	0.04	-	?	?	?	?	0.09	-	0.78 + 0.02	0.01	1.11
+ Cyclo-C_3H_6	0.55	0.14	-	-	-	-	-	-	-	-	0.31	2.22

a) The relative intensities were taken as the ratio of the total band area of the observed spectrum to the total area of all observed emissions (200.0-600.0 nm) adjusted for the response of the detection system as a function of wavelength.

b) Includes the High pressure and Tail bands.

c) Some bands appeared in the He^* + C_2H_4, C_2H_2 reactions which could not be assigned unambiguously and were integrated separately. Also includes continuum from Ar^* + C_2H_2, and the C_6H_6 ($^1B_{2u} \rightarrow {}^1A_{1g}$) molecular spectrum plus some unassigned lines.

d) CH/C_2 is the ratio of the total integrated, corrected emission arising from CH to those from C_2.

e) No emission observed.

f) The C_2(e,d,c, & b) states may be weakly present, but are overlapped by the $C_6H_6^*$ emission. Note that C_6H_6/C_2 + CH $\simeq$ 4.0.

plots and are listed in Table 5. The dissociative excitation channel is only 8% of the total quenching for $He(2^3S) + C_2H_2$ and much less for CH_4, C_2H_4 and cyclo-C_3H_6. The C_2H_2 result was surprising because the flame appears strong to the eye and extensive spectra are obtained from 200-600 nm. Nevertheless, none of the features are really strong and the emission accounts for only 8% of the total quenching. It is interesting to note that the CH(A-X) and C_2(A-X) are dominant in each of the reactions. The H* distributions always decline with increasing quantum number.

The results of this work can be combined with previous studies[7-12] of the ionization pathways to better characterize the distribution of exit channels from $He(2^3S)$ + hydrocarbons. Herman and Cermak[12b] have shown that associative ionization does not compete effectively with Penning ionization. In molecular beam studies[12a], analysis of the positive ions indicated that collision cross-sections for ionizing reactions of polyatomic molecules with $He(2^3S)$ and $He(2^1S)$ were large (on the order of 10 $\AA^2$) and the ionic fragmentation pattern quite extensive.[11] The lack of emission spectra that could be attributed to ionic emission, except for the minor CH^+ from C_2H_2, suggests that the electronically excited states of the ions either fragment or undergo internal conversion before the occurrence of radiative transitions. The negative results of the tests for ion-electron combination spectra suggest that the observed neutral emission must result from predissociation of RH* states formed in the primary process. Table 6 is an attempt to compare the cross-sections for different exit channels of $He(2^3S)$ + hydrocarbon reactions. Since the helium metastables in Ref. 12a consisted of both $He(2^3S)$ and $He(2^1S)$, the data in the first column of Table 6 cannot be compared with the rest on an absolute basis. Also, it should be noted that the absolute cross-sections for total ionization obtained by beam measurements[12a,19] yield consistently higher values than the total quenching cross-sections obtained by flowing afterglow measurements.[4a] The discrepancies, well outside the combined experimental uncertainties, are still not totally explained although the finding of a temperature dependence for the quenching rate constants explains many of the discrepancies.[4b,19] One must, therefore, exercise caution when comparing cross-section data obtained by different methods. However, it is evident that ionizing collisions dominate the total quenching of $He(2^3S)$ by hydrocarbons.

Table 5. Dissociative Excitation Cross-Sections for Quenching $He(2^3S)$

Reactant	σ^*_{He} ($\mathring{A}^2$)[a]	σ total ($\mathring{A}^2$)[b]	$\frac{\sigma^*_{He}}{\sigma \text{ total}}$
CH_4	0.06	9.8[4a]	0.006
C_2H_2	0.97	12[c]	~0.081
C_2H_4	0.27	15[c]	~0.018
cyclo-C_3H_6	0.17	22[c]	~0.008

a. σ^*_{He} is the dissociative excitation cross section determined in this study.

b. σ total is the total quenching cross section for $He(2^3S)$ with HC.

c. Estimated from the correlation with polarizabilities[2] or C_6 coefficients.[1a]

Table 6. Exit Channels of Reactions of Hydrocarbons with $He(2^3S)$

Molecules	Cross-Sections (in units of $\mathring{A}^2$)				
	Beam			Flowing Afterglow	
	Total Ionization (Ref. 12a)	(Ref. 19)	AI/PI[c] (Ref. 12b)	Dissociative Excitation (This Study)	Total Quenching (Ref. 4a)
CH_4	6	27.5	n.d.[a]	0.06	9.8
C_2H_2	19	n.d.	<0.002	0.97	12[b]
C_2H_4	20	n.d.	<0.015	0.27	15[b]
Cyclo-C_3H_6	n.d.	n.d.	n.d.	0.17	22[b]

a. not determined

b. estimated values

c. ratios of associative ionization to Penning ionization cross section.

$He(2^3S) + N_2O$, CO_2 and O_2

The experimental technique described for the hydrocarbons has been extended to study diatomic and triatomic molecules known to give extensive emission in the 190-850 nm spectral range from $He(2^3S)$ reastions. The results of some preliminary investigations are included in Table 7. Emissions from excited parent ions dominate the observed spectra. Weak neutral emission from $N_2(B-A)$ was observed in the He* + N_2O reaction and $CO(a^3\Pi \rightarrow X^1\Sigma^+)$ was observed from $He(2^3S) + CO_2$. Both of these neutral processes are thought to arise from recombination of molecular ions and electrons. However, the atomic lines of oxygen arise from primary interaction between $He(2^3S)$ and O_2[18]. An interesting observation from the N_2O reaction is the appearance of the $N_2^+(B-X)$ emission at high pressures. Formation of $N_2^+(B)$ requires an energy in excess of 19.8eV and we assign this reaction to charge transfer with He^+, giving an N_2O^+ state that predissociates to $N_2^+(B) + O$. The $N_2^+(B)$ vibrational distribution has maximum population at intermediate levels. Detailed interpretation of N_2O^+ and CO_2^+ spectra obtained from $He(2^3S) + CO_2$ and N_2O is planned. Also, additional work will be done to assign cross-sections to emission processes from other molecules reacting with $He(2^3S)$. As soon as the He_2^+ apparatus is operating, the excitation processes from the He_2^+ reactions will be compared with these $He(2^3S)$ reactions.

Table 7. Cross-Sections for Emission from N_2O, CO_2 and O_2.

Reaction Observed		Emission Spectra	Cross-Sections
$He(2^3S) + N_2O$	→	$N_2O^+(\tilde{A}^2\Sigma^+ \rightarrow \tilde{X}^2\Pi)$	5.37 A^{o2}
$He(2^3S) + CO_2$	→	$CO_2^+(\tilde{A}^2\Pi_u \rightarrow \tilde{X}^2\Pi_g)$	13.9 A^{o2}
	→	$CO_2^+(\tilde{B}^2\Sigma_u^+ \rightarrow \tilde{X}^2\Pi_g)$	2.48 A^{o2}
	→	$CO^*(a^3\Pi \rightarrow X^1\Sigma)$[b] + O	0.3 A^{o2}
$He(2^3S) + O_2$	→	$O_2^+(A^2\Pi_u \rightarrow X^2\Pi_g)$	1.29 A^{o2}
	→	$O_2^+(b^4\Sigma_g \rightarrow a^4\Pi_u)$	2.48 A^{o2}
	→	O*(a)	1.61 A^{o2}

(a) Includes oxygen atomic lines observed in the 190-850 nm range.

(b) The CO(a), as well as other CO* states, results from electron combination with $CO_2^+(X)$.

REFERENCES

1. a. L. G. Piper, J. E. Velazco and D. W. Setser, J. Chem. Phys. 59, 3323 (1973).
   b. J. E. Velazco and D. W. Setser, Chem. Phys. Letts. 25, 197 (1974).
   c. L. A. Gundel, D. W. Setser, M. A. A. Clyne, J. A. Coxon and W. Nip, J. Chem. Phys. 64, 4390 (1976).
   d. J. E. Velazco, J. H. Kolts and D. W. Setser, J. Chem. Phys., 65, 3468 (1976).
   e. L. G. Piper, D. W. Setser and M. A. A. Clyne, J. Chem. Phys. 63, 5018 (1975).
   f. D. L. King, L. G. Piper and D. W. Setser, J. C. S. Faraday II, In Press (1976).
2. a. M. Bourene and J. Le Clave, J. Chem. Phys. 58, 1452 (1973).
   b. M. Bourene, O. Dutuit and J. Le Clave, J. Chem. Phys. 63, 1668 (1975).
3. H. J. De Jong, Chem. Phys. Letts. 25, 129 (1974).
4. a. A. L. Schmeltekopf and F. C. Fehsenfeld, J. Chem. Phys. 53, 3173 (1970).
   b. W. Lindinger, A. L. Schmeltekopf and F. C. Fehsenfeld, J. Chem. Phys. 61, 2890 (1974).
   c. T. D. Märk and H. J. Oskam, Phys. Rev. A4, 1445 (1971).
   d. R. C. Bolden, R. S. Hemsworth, M. J. Shaw, and N. D. Twiddy, J. Phys. B3, 61 (1970).
   e. M. Cher and C. S. Hollingsworth, J. Chem. Phys. 50, 4942 (1969).
   f. E. E. Benton, E. E. Ferguson, F. A. Matsen and W. W. Robertson, Phys. Rev. 128 206 (1962).
5. a. J. R. McNeeley, G. S. Hurst, E. B. Wagner and M. G. Payne, J. Chem. Phys. 63, 2717 (1975).
   b. G. S. Hurst, E. B. Wagner and M. G. Payne, J. Chem. Phys. 61, 3680 (1974).
6. a. W. C. Richardson and D. W. Setser, J. Chem. Phys. 58, 1809 (1973).
   b. D. W. Setser, Int. J. Mass Spectrom. Ion Phys. 11, 301 (1973). Some of the excitation reported in this paper arise from He_2^+ or He^+, as well as from $He(2^3S)$.
   c. J. A. Coxon, M. A. Clyne and D. W. Setser, Chem. Phys. 7, 255 (1975).
   d. J. A. Coxon, P. J. Marcoux and D. W. Setser, Chem. Phys., 17, 403 (1976).
7. a. V. Cermak, Coll. Czech, Chem. Comm., 33, 2739 (1968).
   b. V. Cermak and J. B. Ozenne, Int. J. Mass Spectrom. Ion Phys. 7, 399 (1971).

8. H. Hotop, Rad. Research 59, 379 (1974).

9. D. S. C. Yee, W. B. Stewart, C. A. McDowell and C. E. Brion, J. Electron Spectroscopy and Related Phenomenon, 7, 93 (1975).

10. J. A. Herce, J. R. Penton, R. I. Cross and E. E. Muschlitz, J. Chem. Phys. 49, 958 (1968).

11. H. Hotop, A. Niehaus and A. L. Schmeltekopf, Z. Physik 229, 1 (1969).

12. a. V. Cermak and Z. Herman, Coll. Czech. Chem. Comm. 30, 169 (1965).
b. V. Cermak and Z. Herman, Coll. Czech. Chem. Comm. 33, 468 (1968).

13. H. Hotop and A. Niehaus, Int. J. Mass. Spectrom. Ion Phys. 5, 415 (1970).

14. W. B. Hurt and W. C. Grable, J. Chem. Phys. 57, 734 (1972).

15. We measured the total emission intensity from a common upper level v'=0,1 of the CO^+(B-X) and N_2^+(B-X) systems separately. The measured ratios $\Sigma_{v''} I_{v'v''}/I_{v'o}$ compared so well with the calculated scale factors in Table 3 that they justified the subsequent use of these scale factors in obtaining the total emission intensities of CO^+(B-X) and N_2^+(B-X).

16. T. S. Wauchop and H. P. Broida, J. Chem. Phys. 56, 330 (1972).

17. L. G. Piper, J. Gundel, J. E. Velazco and D. W. Setser, J. Chem. Phys., 62, 3883 (1975).

18. W. C. Richardson, Ph.D. Thesis, Kansas State University, 1972.

19. J. S. Howard, J. P. Riola, R. D. Rundel and R. F. Stebbings, J. Phys., B7 376 (1974).

III. Quenching Reactions of Excited Atomic Halogen States ($np^4(n+1)s$) by Molecular Halogens.

J. H. Kolts and D. W. Setser, J. App. Phys., 48, 409 (1977),

Department of Chemistry, Kansas State University, Manhattan, Kansas 66506
(Received 12 July 1976)

The reaction of electronically excited state $Br^*(4p^4, 5s)$ atoms with Br_2 and BrI produces electronically excited Br^*_2, which gives a complex emission system in the 190–350-nm region. In both cases the excitation reaction probably involves bromine atom transfer with formation of Br_2^*. Similar reactions may be expected between other excited $np^4(n+1)s$ halogen atoms and suitable halogen donor molecules. These experiments were done in a flowing-afterglow apparatus at 1–8 Torr; the Br* atoms were generated from interaction of the precursor molecules with metastable argon atoms or with metastable helium atoms. Under high-pressure excitation conditions, formation of Br_2^* by reaction of Br* with Br_2 followed by vibrational relaxation may contribute to the excitation mechanism for the Br_2^* laser system initiated by *e*-beam or discharge pumping of Br_2/Ar mixtures.

PACS numbers: 42.55.Hq, 34.50.Hc, 82.20.Rp, 82.30.Cf

Laser action recently has been observed on the molecular bands of I_2 (342 nm)[1,2] and Br_2 (292 nm).[3,4] The spectroscopic assignments are not well known[5]; however, it is accepted[6,7] that the upper state is of the ionic type and that the lower state probably is a member of the first excited triplet manifold. We shall denote the upper state with an asterisk without attempting a more definitive identification. The mechanism(s) for producing the upper state in the discharge of e-beam-pumped argon/halogen mixtures is not established.[1-4,6,8] In this work we have investigated the reaction between excited $Br^*(5s)$ atoms and Br_2, which has been suggested[4] as an excitation mechanism,

$$Br^*(5s\,{}^4P_J, {}^2P_J) + Br_2 \rightarrow Br_2^* + Br. \qquad (1)$$

Based upon the observation of Br_2^* emission, reaction (1) does provide a possible way for forming Br_2^*. A similar reaction also was found between $Br^*(5s)$ and BrI.

The experiments utilized a low-pressure (1—8 Torr) flowing-afterglow apparatus. Metastable argon (the ratio of $^3P_2/^3P_0$ is ~6:1) or metastable He($2\,^3S$) atoms were produced by flowing prepurified argon or helium through a hollow cathode discharge.[9,10] The reagents were added coaxially to the flow of metastable argon atoms a few milliseconds after the discharge. Emission from 190 to 800 nm was observed with a 0.75-m Jarrel-Ash monochromator fitted with a photomultiplier tube and a SSR photon counting rate meter. Previous studies[10] of the $Br_2 + Ar(^3P_2)$ reaction have established the quenching rate constant of $Ar(^3P_2)$ by Br_2, 66×10^{-11} $cm^3\,molecule^{-1}\,sec^{-1}$, and the main primary productions, as shown in reaction (2):

$$\begin{aligned} Ar(^3P_2) + Br_2 &\rightarrow ArBr^* + Br \\ &\rightarrow Ar + Br^*(5s) + Br \\ &\rightarrow Ar + Br^*(5s''). \end{aligned} \qquad (2)$$

The $Br^*(5s)$ and $Br^*(5s'')$ are thought to be formed via predissociation of the initially formed ArBr*. The $Br^*(5s)$, which have the distribution

$$^2P_{1/2} : {}^2P_{3/2} : {}^4P_{1/2} : {}^4P_{3/2} : {}^4P_{5/2}$$
$$= 0.12 : 0.20 : 0.11 : 1.0 : 0.80$$

constitute more than 98% of the observed emission. Some very weak Br_2^* emission in the 200—300-nm region

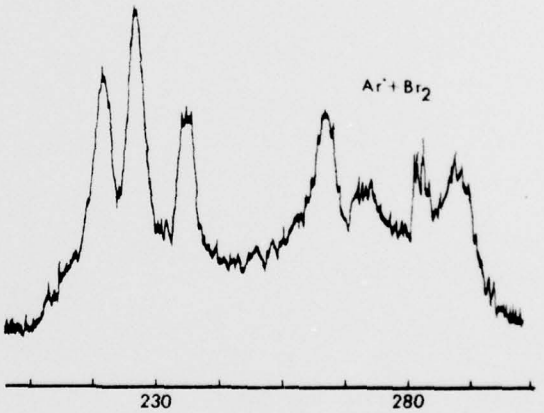

FIG. 1. Spectra from $Ar^*(^3P_{0,2}) + Br_2$. The bromine flow was 4.5 μmol min^{-1} (corresponding to a concentration of 4.8×10^{12} molecules cm^{-3}) with a flow tube pressure of 3.3 Torr. Full scale corresponds to 3000 on the rate meter; the spectrometer slit width was 100 μ.

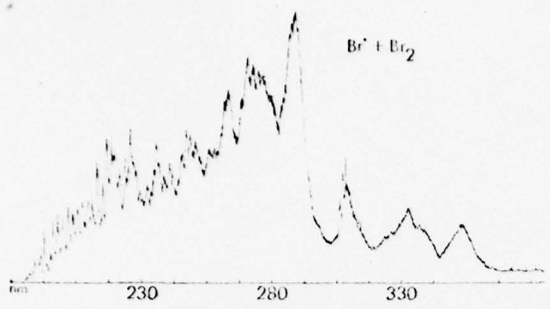

FIG. 2. Spectra from $Br^*(5s) + Br_2$. The bromine flow was 187 μm min^{-1} (corresponding to a concentration of 1.9×10^{14} molecules cm^{-3}) with a flow tube pressure of 3.4 Torr. Full scale corresponds to 30 000 on the rate meter; the spectrometer slit width was 100 μ. The sharp features on the band at 310 nm is $OH(A\text{-}X)$ from the $Ar(^3P_{0,2}) + H_2O$ (impurity) reaction.

(see Fig. 1) also seems to be directly produced, but this emission contributes less that 0.5% to the yield of excited-state products.

In the present work high flows of Br_2 were used in order to intercept the $Br^*(5s)$ atoms before radiative decay (in the vacuum ultraviolet). The Br_2^* emission spectrum that was obtained under the high flow conditions is shown in Fig. 2. The difference between Figs. 1 and 2 is quite obvious, and secondary reactions clearly must contribute to the Br_2^* excitation for high flow conditions. The spectrum in Fig. 2 is very complex; but the most intense feature is the broad band at ~290 nm which is close to the laser transition.[3,4] The variation of the Br_2^* emission intensity versus Br_2 flow suggested that the formation mechanism for the spectrum of Fig. 2 was a secondary reaction of Br^* with Br_2. This mechanism was confirmed by reacting a high flow of BrI with $Ar(^3P_{0,2})$, and obtaining an emission spectrum similar to that of Fig. 2. With BrI, an I_2^* emission system, peaking at 342 nm, also was observed. For further confirmation, Br_2 was reacted with $He(2\,^3S)$; the primary reaction yields excited-state Br^* atoms, as well as Penning ionization.[11] For high Br_2 flows, a Br_2^* emission spectrum strongly resembling that of Fig. 2 was obtained. Since the distributions of atomic Br^* states are not identical for the $He(2\,^3S)$ and $Ar(^3P_{0,2})$ reactions, the two Br_2^* emission spectra need not be exactly the same. Experiments also were done in which CF_3Br and HBr were reacted with $Ar(^3P_{0,2})$. With CF_3Br a weak emission in the 190–250-nm range was observed. An extended weak emission (200–300 nm) was observed with HBr, which may be analogous to the many-lined HCl^* continuum observed from $Ar(^3P_{0,2})$ with HCl.[12] The emissions from HBr and CF_3Br apparently result from primary interactions with $Ar(^3P_2)$. The failure to form Br_2^* could be either that $Br^*(5s)$ is not produced in the primary reaction or that Br^* does not react efficiently with CF_3Br and HBr, which have higher bond energies than Br_2 or BrI, to form Br_2^*.

Attempts were made to obtain a spectrum of the Br_2^* emission at higher pressures in order to simplify the appearance of the spectrum. However, no relaxation was observed over the 1–8-Torr region, which implies that the radiative lifetime of Br_2^* is <50 nsec. Unfortunately, the spectrum of Fig. 2 is not sufficiently resolved to permit band assignments, although on a qualitative basis there is a resemblance to the Br_2 spectra excited in an Ar/Br_2 discharge.[6] A further complication is that the emission may be a combination of bound-bound and bound-free spectra.[13,14]

The electronic quenching of $Br(5s\,^4P_{5/2})$ has been studied by Bemand and Clyne.[15] The cross sections are <0.04 Å^2 for Ar and 146 Å^2 for Br_2. Since the radiative lifetime[15] of the $^4P_{5/2}$ state ($\sim5\times10^{-7}$ sec) is an order of magnitude larger than for $^4P_{1/2}$ and two orders of magnitude larger than for the other three states, Bemand and Clyne could only study quenching of the $^4P_{5/2}$ state. In our experiments $[Ar, {}^3P_{0,2}] = 5\times10^{19}$ cm^{-3} and the [Br] concentration can be no larger than twice that of $Ar(^3P_{0,2})$. Therefore, radiative trapping of the $Br^*(5s)$ states will be unimportant. Under our experimental conditions, $[Br_2] = 5\times10^{12}$–5×10^{14} molecules cm^{-3} and mainly the Br^* state with the longest lifetime ($^4P_{5/2}$) will react with Br_2. Fortunately, the branching ratio for formation of Br_2^* by reaction (2) must be relatively high, and observation of the Br_2^* emission from quenching of $Br^*(5s)$ was possible.[16]

The ionization potential of $Br^*(5s)$ is 4.0 eV. Therefore, interaction between $Br^*(5s)$ and reagents with large electron affinities can occur by an ionic-covalent curve-crossing mechanism in the same way as the reactions of metastable rare-gas atoms or alkali-metal atoms with such reagents.[10] The large quenching rate constants and selectivity for formation of the ionic molecular excited states in the quenching of the resonance atomic halogen states by halogen-containing molecules can be understood in terms of this mechanism. The $Cl^*(4s)$ states have longer lifetimes than the $Br^*(5s)$ states and reactions analogous to reaction (1) would be expected. Unfortunately, the primary interaction of $Ar(^3P_{0,2})$ with many chlorine-containing compounds[10] either produces Cl_2^* directly or does not form $Cl^*(4s)$ because of energy restrictions, and experiments with $Ar(^3P_{0,2})$ for investigation of the $Cl^* + RCl$ reaction (R = polyatomic group) were inconclusive. However, reaction of $He(2\,^3S)$ with Cl_2 does give the Cl_2^* 260-nm continuum. Since $Cl^*(4s)$, as well as $Cl_2^*(A)$, are known primary products,[17,18] the excitation of the Cl_2^* state may involve reaction of $Cl^*(4s)$ with Cl_2. The radiative lifetimes of the $I^*(6s)$ atoms are too short for the reactions between I^* and RI molecules to be studied easily by the technique used in this work. Nevertheless, a very weak I_2^* emission was observed from $Ar(^3P_{0,2})$ with BrI and CF_3I.

The interaction between argon metastable atoms (and probably the diatomic argon excimer states) and bromine- and iodine-containing molecules have large rate constants and high branching ratios for formation of electronically excited bromine and iodine atoms. The present work indicates that the subsequent reactions between the excited state ($np^4, n+1s$) halogen atom and halogen-containing molecule are rapid and may have appreciable branching ratios for formation of excited states of the molecular halogens. Therefore, the deposition of energy in mixtures of argon with bromine- or iodine-containing molecules provides an efficient way for forming the ionic excited states of the molecular

halogens. Further work is needed to establish assignments for the upper and lower molecular states and to measure the rate constants for their quenching and vibrational relaxation.

†Research supported by the Advanced Research Projects Agency of the Department of Defense and monitored by ONR under contract No. N00014-76-C-0380.

[1]J.J. Ewing and C.A. Brau, Appl. Phys. Lett. 27, 557 (1975).
[2]R.S. Bradford, Jr., F.R. Ault, and M.L. Bhaumik, Appl. Phys. Lett. 27, 546 (1975).
[3]J.R. Murray, J.C. Swingle, and C.E. Turner, Jr., Appl. Phys. Lett. 28, 530 (1970).
[4]J.J. Ewing, J.H. Jacob, J.A. Mangano and H.A. Brown, Appl. Phys. Lett. 28, 656 (1976).
[5]J. Tellinghuisen (private communication).
[6]M.V. McCusker, R.M. Hill, D.L. Huestis, D.C. Lorents, R.A. Gutcheck, and H.H. Nakano, Appl. Phys. Lett. 27, 363 (1975).
[7]K. Wieland, J.B. Tellinghuisen, and A. Nobs, J. Mol. Spectrosc. 41, 69 (1972).
[8]C.H. Chen and M.G. Payne, Appl. Phys. Lett. 28, 219 (1976).
[9]D.W. Setser, D.H. Stedman, and J.A. Coxon, J. Chem. Phys. 53, 1004 (1970).
[10]L.A. Gundel, D.W. Setser, M.A.A. Clyne, J.A. Coxon, and W. Nip., J. Chem. Phys. 64, 4390 (1976).
[11]L.A. Gundel, M.A.A. Clyne, and D.W. Setser (unpublished).
[12]See Ref. 10 for a description of the HCl* emission from $Ar(^3P_{0,2}) + HCl$. The HBr* emission strongly resembles that from the HCl reaction.
[13]M.F. Golde, J. Mol. Spectrosc. 58, 261 (1975).
[14]J.B. Tellinghuisen, Chem. Phys. Lett. 29, 359 (1974).
[15]P.P. Bemand and M.A.A. Clyne, J. Chem. Soc. Faraday Trans. 2 68, 1755 (1972).
[16]Absorption of the atomic Br* vacuum uv emission by Br_2 gives a Br_2^* molecular resonance series in the 155–187-nm region [M.A.A. Clynne and H.W. Cruse, J. Chem. Soc. Faraday Trans. 2 68, 1281 (1972)]. Absorption of the Br* radiation may contribute to the Br_2^* excitation in the 200–350-nm region under some conditions. This, however, should be negligible for the experimental conditions for which Fig. 2 was obtained.
[17]P.P. Bemand and M.A.A. Clyne, J. Chem. Soc. Faraday Trans. 2 71, 1132 (1975).
[18]W.C. Richardson and D.W. Setser, J. Chem. Phys. 58, 1809 (1973).